ANNALI DI GEOFISICA, VOL. XXXVII, N. 6, December 1994

Positive and negative feedback in the earthquake cycle: the role of pore fluids on states of criticality in the crust

Ian G. Main([1]), **Philip G. Meredith**([2]), **Jeremy R. Henderson**([1]) ([3]) **and Peter R. Sammonds**([2])
([1]) *Department of Geology and Geophysics, University of Edinburgh, Grant Institute, Edinburgh, U.K.*
([2]) *Department of Geological Sciences, University College London, U.K.*
([3]) *Present address: Department of Geological Sciences, University of Durham, U.K.*

Abstract
Fluids exert a strong physical and chemical control on local processes of rock fracture and friction. For example they may accelerate fracture by stress corrosion reactions or the development of overpressure (a form of positive feedback), or retard fracture by time-dependent stress relaxation or dilatant hardening (negative feedback), thereby introducing a variable degree of local force conservation into the process. In particular the valve action of dynamic faulting may be important in tuning the Earth to a metastable state of incipient failure on all scales over several cycles, similar to current models of Self-Organised Criticality (SOC) as a paradigm for earthquakes. However laboratory results suggest that ordered fluctuations about this state may occur in a single cycle due to non-conservative processes involving fluids which have the potential to be recognised, at least in the short term, in the scaling properties of earthquake statistics. Here we describe a 2-D cellular automaton which uses local rules of positive and negative feedback to model the effect of fluids on failure in a heterogeneous medium in a single earthquake cycle. The model successfully predicts the observed fractal distribution of fractures, with a negative correlation between the predicted seismic *b*-value and the local crack extension force *G*. Such a negative correlation is found in laboratory tests involving (a) fluid-assisted crack growth in tension (b) water-saturated compressional deformation, and (c) in field results on an intermediate scale from hydraulic mining-induced seismicity – all cases where *G* can be determined independently, and where the physical and chemical action of pore fluids is to varying degrees a controlled variable. For a finite local hardening mechanism (negative feedback), the model exhibits a systematic increase followed by a decrease in the seismic *b*-value as macroscopic failure is approached, similar to that found in water-saturated laboratory tests under controlled «undrained» conditions, and where dilatancy hardening is independently known to be a local mechanism of negative feedback. A similar pattern is suggested from selected field observations from natural seismicity, albeit with a lesser degree of statistical significance.

Key words *self-organised criticality – fractals – fluid-rock interactions – seismicity*

1. Introduction

For many years one of the most basic and universal properties of earthquake populations – the log-linear Gutenberg-Richter frequency-magnitude law – remained a practical observation which lacked a good scientific explanation. The implied scale-invariance of earthquake source dimension is also found elsewhere in physics, for example in populations of melt fraction or aligned magnetic moment near a critical point (Bruce and Wallace, 1989). However these critical phenomena occur under precise external conditions which require exact

tuning of state variables such as the pressure and/or temperature, in contrast to the more or less universal observation of power-law scaling in earthquake populations in different tectonic provinces with variable heat flow, strain rate, geological composition, age and the ratio of seismic to aseismic deformation. This conundrum has recently been resolved by the suggestion that earthquakes are an example of a Self-Organised Critical (SOC) phenomenon, where after an initial transient settling-in period, the external variables (external stress in response to a constant strain rate) reach a metastable critical point, near failure everywhere, where long-range order may result from strong local interactions due to internal stress concentration (Bak and Tang, 1989; Sornette and Sornette, 1989), and where avalanches of events occur on all scales. In particular cellular automata have been developed which model the macroscopic scaling properties of faults and fault systems using constitutive laws based on rock fracture or friction, the literature being dominated by the Burridge-Knopoff (1967) spring-block frictional slider model with velocity-weakening constitutive laws (*e.g.* Carlson and Langer, 1989). A mature description of faulting and earthquakes as a self-organised critical phenomenon, using a resistor network model of elastic elements and including long-range interactions, is given by Sornette *et al.* (1994a,b).

In all of these models the Earth's brittle crust is assumed to be dry, or that pore fluid pressure and chemistry plays only a peripheral role in the nucleation process. It is our contention that the geological evidence for the activity of pore fluids is sufficiently compelling to require an investigation of their influence on the state of criticality. For example we show here that pore fluids may be active in (a) attracting the overall system to a metastable state near failure over several cycles through the valve action of faulting and (b) producing ordered fluctuations in the scaling exponents in a single cycle. The fluctuations in scaling exponent are modelled with a cellular automaton based on the rules of fracture mechanics, with a feedback rule which includes the effect of local dilatancy hardening prior to microcrack coalescence as a fault nucleation mechanism. The model accounts for the observed behaviour in laboratory tests with servo-control of constant strain rate under the «undrained» conditions (constant pore fluid mass in the deforming sample). To place this work in context we first review the various observations and attempted modelling of the earthquake frequency-magnitude distribution over several cycles, and then examine the evidence for fluctuations in the scaling exponents in a single cycle.

2. Statistical mechanics of earthquakes

If earthquakes were a thermodynamic system at equilibrium, then we might expect their statistical mechanics to reflect a Boltzmann (exponential) distribution of energy transitions

$$p(E)\,dE = A \exp(-E/E^*)\,dE \qquad (2.1)$$

where p is a probability density of earthquakes radiating an energy E, and by analogy E^* might represent the effect of a «tectonic temperature», with greater relative occupancy of the higher energy states for higher E^*. In the familiar world of open thermodynamic systems at equilibrium E^* is always positive, so that p always decreases with increasing E. However in closed systems far from equilibrium the system may be driven to a state where p becomes independent of E, implying infinite E^*, or even to a more energetic state ($E^* > \infty$) where p increases with E, implying negative E^* (*e.g.* see the discussion in Mandl, 1988, section 3.4. for the case of paramagnetism). These three possibilities are illustrated for a simple two-level system in fig. 1a-c. None fits in with the general observation of power-law scaling

$$p(E)\,dE = A\,E^{-(B-1)} \qquad (2.2)$$

usually expressed in seismology as the Gutenberg-Richter frequency-magnitude law

$$\log_{10} N(m) = a - b(m - m_c) \qquad (2.3)$$

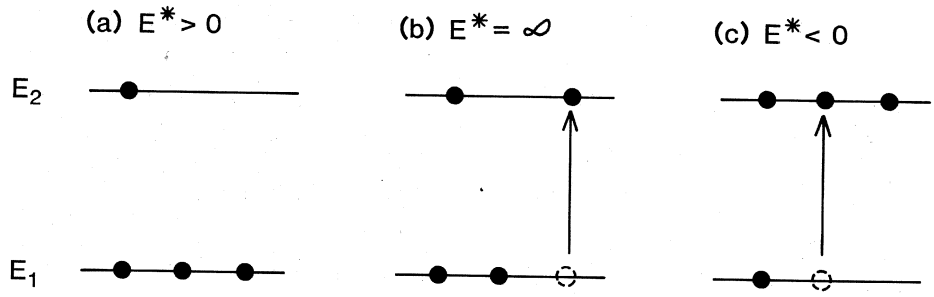

Fig. 1a-c. A schematic diagram of the occupancy of energy states at different E^* for a Boltzmann distribution of energy $p\,(E)\,dE = A \exp(-E/E^*)\,dE$ in a closed system of two energy states with no degeneracy (replication) of either state: a) under normal conditions E^* is finite and positive implying a greater probability of occupancy of the lower energy state E_1, similar to thermodynamic systems; b) as the external energy is increased the probability of occupation becomes equal in both states implying $E^* = \infty$; c) as the supply of external energy increases further occupancy of the higher energy state E_2 exceeds the ground state E_1, implying negative E^*.

where

$$\log_{10} E = cm + d \qquad (2.4)$$

The *frequency*

$$N(m,\, \delta m) = N_T \int_{m-\frac{\delta m}{2}}^{m+\frac{\delta m}{2}} p\,(m')\,dm' \qquad (2.5)$$

is the number of times an earthquake of magnitude in the arbitrary range $(m - \delta m/2,\ m + \delta m/2)$ occurs in a unit time interval, N_T is the total number of earthquakes per unit time interval in the catalogue above the threshold m_c, and a, b, c and d are scaling constants. Earthquake statistics are often presented as a *cumulative frequency*

$$N_C\,(M > m) = N_T \int_m^{\omega} p\,(m')\,dm' \qquad (2.6)$$

where ω is the maximum magnitude. Cumulative statistics are inherently smoother, and are useful in seismic hazard analysis, but they may obscure the detail of earthquake recurrence at high magnitudes where ω is finite (Main, 1992). For example fig. 2 shows that fractal scaling in the *frequency* distribution produces parallel scaling with the *cumulative frequency* with the same negative slope $b = B/c$ at low magnitudes, but results in curvature at high magnitudes as the cumulative frequency rolls off below this trend.

Main and Burton (1984) derived a generalised relation combining the constraints of finite energy with the availability of progressively more replication (degeneracy) of smaller energy transitions, thereby combining (2.1) and (2.2) in the form

$$p\,(E)\,dE = AE^{-(B-1)} \exp(-E/E^*)\,dE\,. \qquad (2.7)$$

This results in a generalised gamma distribution (*e.g.* Kagan, 1993) after integration

$$P(E) = \int_E^{E_{\max}} p\,(E')\,dE' \qquad (2.8)$$

with the constraints of finite mean energy

$$<E> = \int_E^{E_{\max}} E' p\,(E')\,dE' \qquad (2.9)$$

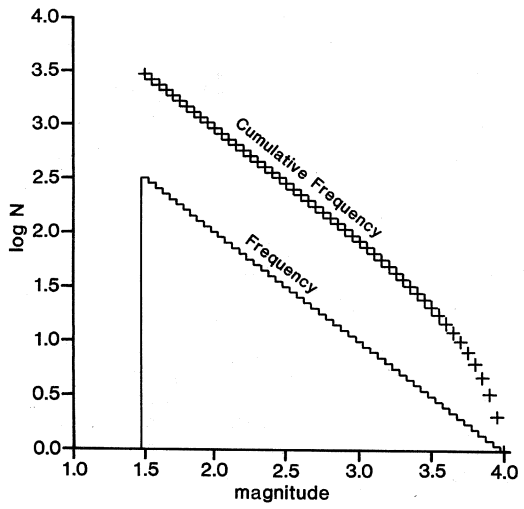

Fig. 2. A schematic diagram of the differences in earthquake statistics for the case of an ideal Gutenberg-Richter law. A straight line in the *frequency* distribution implies curvature at high magnitudes in the *cumulative frequency*. At low magnitudes the two lines are parallel.

and unit total probability

$$P(E_{\min}) = \int_{E_{\min}}^{E_{\max}} p(E')\,dE' = 1\,. \qquad (2.10)$$

The same approach may be adopted for the seismic moment M_0, except that the scaling parameter d is different (Kanamori, 1978). The seismic moment formulation allows a maximum entropy fit simultaneously to the two independent constraints of (a) mean magnitude $< m >$ from the short-term earthquake catalogue and (b) the long-term seismic moment release rate $\dot{M}_0$ via (Main and Burton, 1984, 1986)

$$< M_0 > = \int_{M_0}^{M_0^{\max}} M'_0\, p(M'_0)\,dM'_0 = \frac{\dot{M}_0}{N_T} \qquad (2.11)$$

and

$$< m > = \int_{m}^{\omega} m'\, p(m')\,dm'\,. \qquad (2.12)$$

The gamma distribution (a power law in energy or moment with an exponential tail at high magnitudes) fits large data sets well, for example the earthquake magnitude catalogue in the Mediterranean area (Main and Burton, 1984) and the Harvard moment catalogue for the whole Earth (Kagan, 1993). By «large» in this context we mean areas which have a spatial extent much larger than the biggest earthquake rupture, so that $0 < E^* \ll E_{\max}$, where $E_{\max}$ represents the energy of an event which would break across the whole area of interest. For catalogues with spatial dimensions more similar to the largest earthquake (*e.g.* Southern California) the form (2.2) holds, implying a power-law (fractal) distribution with $E^* \approx E_{\max}$ or effectively $E^* = \infty$. By analogy with fig. 1b, this merely implies a distribution with an equal probability of occupancy of each available energy level, so that the hierarchy of fault elements fails exactly once in each cycle, a property also used by Rundle (1989) to derive the Gutenberg-Richter law.

If the system is overdriven, *i.e.* there is actually an increase in the probability of occupancy as we go to higher energy levels, then we would expect a «characteristic» size effect, with larger earthquakes being more common than expected from extrapolating the fractal trend of the smaller events, implying negative E^*. This state is characterised by a progressively greater occupancy of the higher available energy states as in fig. 1c. By «characteristic» we merely imply a peak in the probability of a population of earthquakes, rather than the exact repetition of individual events. A characteristic peak is seen in the percolation model for seismogenesis developed by Lomnitz-Adler (1985, 1988) and in the cellular automaton of Ben-Zion and Rice (1993), which applies a depth-dependent constitutive behaviour to a 2D fault plane embedded in an otherwise elastic medium, loaded from the side by tectonic forces, and through an underlying ductile lower crust. Such a characteristic peak at scales limited only by the size of the model is also seen in other examples of percolative phenomena, and is known as a state of «supercriticality» in the percolation literature (Stauffer, 1985).

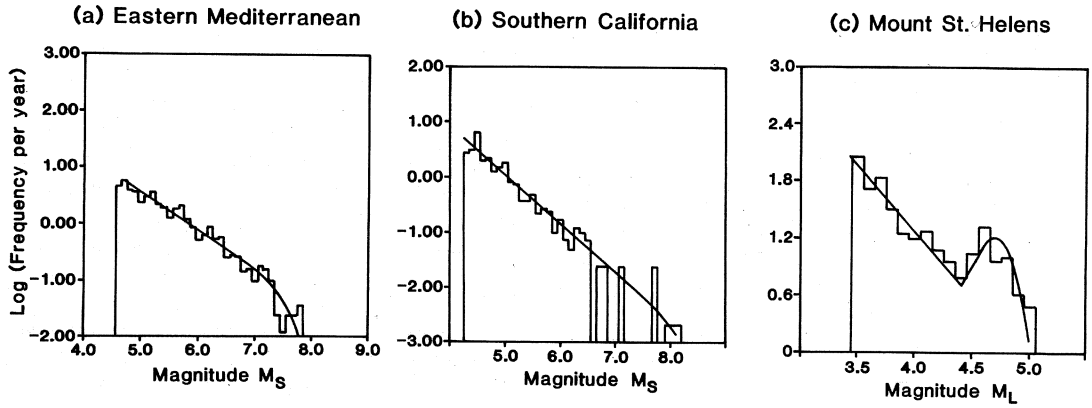

Fig. 3a-c. Frequency-magnitude distributions corresponding to examples of the generalised gamma distribution of equation (2.7) with (a) positive, (b) infinite and (c) negative E^* for field data from (a) the Eastern Mediterranean, (b) Southern California and (c) Mount St. Helens, Washington. The original data are presented in Main and Burton (1984) and Main (1987).

Characteristic size effects are often reported in earthquake frequency-magnitude statistics from catalogues dominated by single faults or fault segments, and where the historical or geological record contains a sufficient number of events at high magnitude to see the effect (Schwartz and Coppersmith, 1984; Ward, 1992). The 1980 eruption of Mount St. Helens also produced a strong, statistically significant characteristic peak due to the narrowing of the brittle zone to 2 km by the raised isotherms above the magma chamber, limiting earthquakes to a characteristic magnitude of 5 or so (Main, 1987). The latter example is a good illustration of the a finite, overdriven or «supercritical» system, where the rate of energy input from magma injection exceeded the ability of a finite fractal hierarchy of faults to dissipate the available energy by a single event in each cycle.

Figure 3a-c shows type examples from field data of the different forms of the frequency-magnitude distribution predicted by eq. (2.7) for (a) positive, (b) infinite and (c) negative E^*. A similar range of possibilities for the frequency-magnitude distribution at high magnitudes (*i.e.* (a) exponential – (b) fractal – (c) characteristic) is seen in several of the more recent cellular automata modelling earthquakes (Lomnitz-Adler, 1993; Rundle and Klein, 1993) and in the frequency-volume statistics of avalanche processes in general (Ceva, 1993; Carlson *et al.*, 1993). For the earthquake slider-block models true SOC emerges only for systems exhibiting weak annealed (*i.e.* permanent) heterogeneity in the strength of individual elements (Rundle and Klein, 1993), or for those exhibiting low (partial) stress drop (Lomnitz-Adler, 1993). For «critical» systems where these conditions do not hold, the sensitivity of these models to external conditions such as the driving plate velocity (Rundle and Klein, 1993) implies that they are not strictly SOC phenomena. SOC only emerges for low heterogeneity (or low local stress drop), where the behaviour is fractal with a scaling exponent b or B independent of the external conditions (Sornette *et al.*, 1994b).

3. Fluctuations in scaling exponents

We have seen above that the form of the frequency-magnitude distribution – averaged over *several* cycles of macroscopic failure – may vary according to the rate of external energy input compared to the available area for energy dissipation in a single cycle of macro-

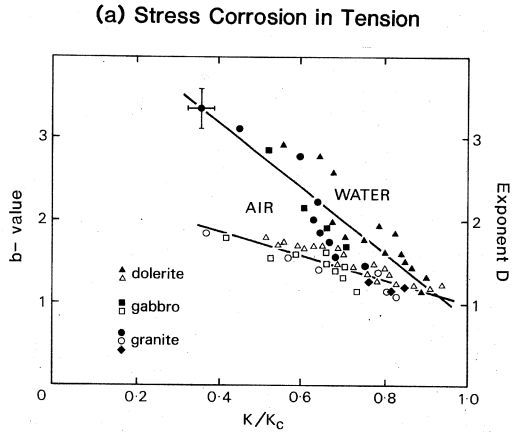

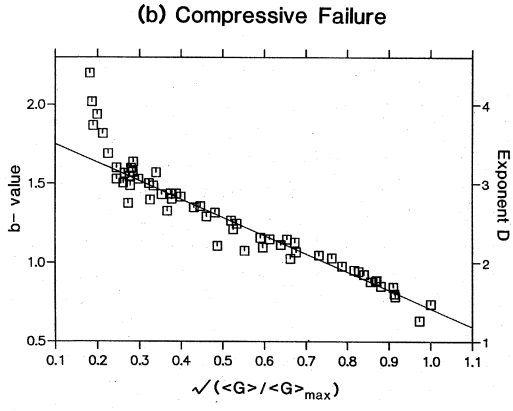

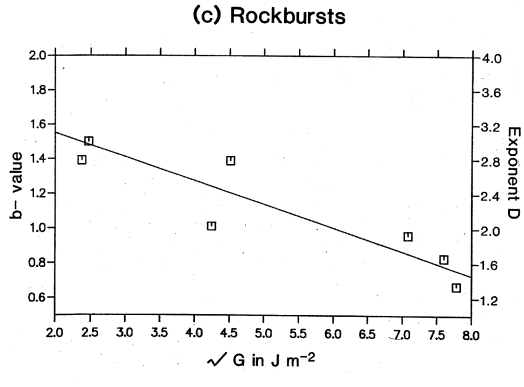

scopic failure. SOC is only seen when no strong characteristic length is present, when the initial strength heterogeneity is either not strong or not persistent, and when the largest earthquake just percolates across the entire area of interest in a single cycle. Under these conditions the behaviour is fractal, with a universal, time-independent scaling exponent corresponding to $b \approx 1$. However systematic fluctuations in b-value are sometimes associated with individual large earthquakes (Smith, 1980, 1986), often associated with temporal changes in scattering attenuation (Jin and Aki, 1986) or fractal clustering of epicentres (Henderson *et al.*, 1992). There are two models which may explain this ordered fluctuation, by (a) systematic fluctuations in external conditions (stress, strain or moment rate applied to the model boundary) for the case of strong heterogeneity (*e.g.* Rundle and Klein, 1993), or (b) fluctuations in the local degree of conservation of force in non-conservative cellular au-

Fig. 4a-c. Systematic variations of the seismic b-value with the crack extension force G for the case of: a) quasi-static crack growth by stress corrosion under tensile loading in the laboratory (Meredith and Atkinson, 1983; Meredith *et al.*, 1990), where K is the stress intensity, K_c is the fracture toughness and $K \propto \sqrt{G}$ (Atkinson, 1987); b) microcrack growth prior to compressional failure under experimental conditions of constant pore fluid mass, and where the mean crack extension force $< G >$ is inferred from a modified Griffith criterion for fractal damage (Main, 1991; Main *et al.*, 1993); and c) hydraulic mining-induced seismicity, after Xie and Pariseau (1991), original data from Sato *et al.* (1986), where G was measured from the total seismic energy released divided by the total mined-out area producing the rock debris. In (a) and (c) the b-value was estimated by least squares, and in (b) by the maximum likelihood technique. The magnitude scales are equivalent throughout since the acoustic emission magnitudes (in dB) in (a) and (b) were divided by a factor 20 to obtain an equivalent M_L to that used by Sato *et al.* (1986). For comparison with the results of (a), those in (b) and (c) are plotted against $\sqrt{G}$, and the y-axis also shows the exponent D of the crack length distribution, so that $B = D/3$ or $b = D/(3c)$.

tomata for weak heterogeneity (*e.g.* Olami *et al.*, 1992). Such fluctuation in *individual* cycles may also be allowed in a state of SOC as long as the *average* properties over several cycles are preserved.

In the cellular automaton model of Olami *et al.* (1992) a negative correlation is found between the seismic *b*-value and the degree of conservation, 4α, measured by the fraction of force redistributed to the 4 nearest neighbours after a single element fails, so that $0 < 4\alpha < 1$. *b*-values near 1 are only produced in this variant of the Burridge-Knopoff model when $4\alpha \approx 0.8$, implying a finite amount (20%) of anelastic dissipation (non-conservation of local force). Figure 4a-c (after Main *et al.*, 1994) shows three examples of a similar negative correlation between *b* and an independently-measured Griffith crack extension force, defined by $G = \partial U/\partial A$, where U is the external mechanical energy and A is the crack surface area. In all of these examples – laboratory tests in tension or compression, and field results from hydraulic mining-induced seismicity – the mechanism of non-conservation is known to involve the physical or physico-chemical activity of pore fluids. The results all suggest that the greater the degree of local force conservation (higher G), the greater the potential for a larger avalanche in an individual event, and the lower the *b*-value of the population as a whole.

Effective dissipation of the normalised crack extension force G/G_c may occur by physico-chemical effects such as stress corrosion (Atkinson and Meredith, 1987), or by crack blunting in the form of a plastic «process zone» of distributed damage ahead of the crack tip (Barenblatt, 1962). In both cases an individual fracture may propagate quasi-statically at values less than the value G_c for the dynamic failure of the specimen of interest (usually this is called «subcritical» crack growth ($G < G_c$) as opposed to «critical» ($G = G_c$) but here we shall refer to these phenomena respectively as «quasi-static» or «dynamic» crack growth to avoid possible confusion with critical point phenomena). The parameter which matters is not the absolute value of G, but its relative value G/G_c, because G_c tends to increase with fracture size, from 1 J m^{-2} in laboratory fracture to 10^4 J m^{-2} in earthquakes (Scholz, 1990). Fluctuations in the conservation parameter $0 < G/G_c < 1$ due to local time-dependent processes could in principle produce ordered fluctuations about the state of criticality with predictive power at least in the short term in an individual cycle (in practice a minimum value of G/G_c above 0 will be required for physico-chemical processes with a finite activation energy; Atkinson and Meredith, 1987). Unfortunately, the quantity and quality of the data presently available, even in earthquake zones of very low seismic attenuation and good signal to noise ratio, are often insufficient to allow the unequivocal observations of such precursors before (or even after) any major event (Scholz, 1990).

The above discussion has shown that a wide variety of local processes produce the same overall statistical properties on a macroscopic scale, so that the models so far produced do not always have strong powers of discrimination. For example in all of the models large events in the form of runaway «avalanches» are produced due to strong positive feedback between the failure of one element and the immediate loading of its neighbours. Nevertheless, most models are forced to introduce some arbitrary form of negative feedback, in the form of finite anelastic dissipation at a local scale, in order to account for the observed scaling exponents of natural seismicity (particularly the seismic *b*-value). In the next section we consider more explicitly the influence of pore fluids on the mechanisms of feedback in the crust, and their potential to introduce ordered fluctuations about the state of SOC.

4. Influence of pore fluids

4.1. *Over several cycles*

Earthquakes occur because of slip on faults loaded at a relatively constant strain or moment rate by plate tectonics. Faults also act as conduits for fluids (Sibson, 1977, 1981), produced either by metamorphic reactions in the lower crust and mantle (Kerrich, 1986), or by

the recycling of water subducted in wet sediments and in hydrous mineral phases (Nur and Walder, 1992). The relative impermeability of crystalline rock, and the possibility of pressure seals on fault walls, implies that pore pressures may become elevated above hydrostatic to values approaching lithostatic at depths in excess of a few km, as often seen in the prospecting for hydrocarbons (Sibson, 1990). This is consistent with the relatively small changes in effective stresses which are required (of the order 1 bar or 0.1 MPa), for example due to pore pressure changes during hydrocarbon extraction or dam impoundment, to induce earthquakes in the upper crust on timescales of 5-10 years or so (Segall, 1989; Scholz, 1990). It is however important to recognise that the trigger here is not just the simple poroelastic effect illustrated in fig. 5, but the effect of *local* changes in p inducing additional stresses as the surrounding volume of rock collapses into (or expands from) the resulting pressure draw-

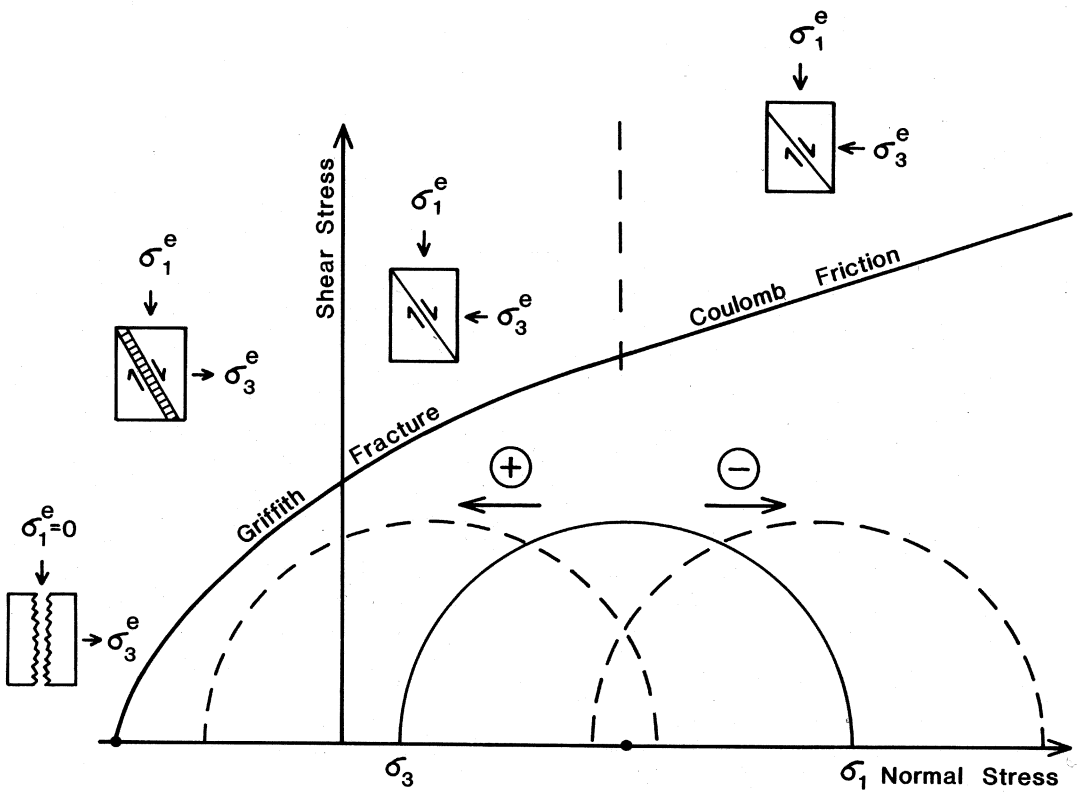

Fig. 5. A simple diagram showing the mechanical effect of a change in pore-fluid pressure on the likelihood of failure, using the Mohr circle concept with the predicted Griffith failure curve at low confining stress and Coulomb friction at higher stresses. If the pore pressure p increases the effective stresses are reduced to $(\sigma_1 - p, \sigma_3 - p)$, the Mohr circle moves nearer to failure envelope and a mechanism involving some opening displacement. This is an example of positive feedback, and is important in the valve action of faulting. If the pore pressure reduces, say because of local dilatancy, the Mohr circle moves away from the failure curve, implying a negative feedback.

down or increase. For example the seismicity induced during hydrocarbon extraction tends to be above and below the reservoir volume rather than inside it (Segall, 1989).

Although the explicit presence of pore fluids is not required to produce SOC, there is compelling evidence that fluids do exert a strong control on the local dynamics in the Earth. For example Rice (1992) showed that the relative and absolute weakness of the San Andreas fault could be attributed to fluid overpressure on the fault, both compared to the hydrostatic value and to that of the surrounding country rock. This suggestion has recently been confirmed by Chester *et al.* (1993), who examined fault gouge from boreholes drilled through the San Andreas fault. Direct evidence for fluid overpressure at earthquake nucleation depths comes from the presence of hydrothermal veining (Sibson *et al.*, 1988), and from fluid trapped in inclusions in fault rocks under conditions characteristic of the middle crust (Hodgkins and Stewart, 1994). The rate of fluid pressure build-up on earthquake faults in the fold and thrust belt of the transverse ranges of California has been estimated as about 0.1 bar per year (Keller and Loaciga, 1993), quite significant compared to the few tens of bars involved in coseismic slip in general, and quite sufficient to explain the recurrence times of earthquakes in this particular area. All of these recent quantitative studies suggest that fluid overpressure is a more than plausible mechanism of moving the crust to a state of SOC, although none of these effects have been explicitly included into any of the critical models for seismogenesis described above.

A full solution of the coupled poroelastic problem requires models which reflect a simultaneous dynamic balance between (a) the input and release of tectonic strain energy, and (b) fluid flux into and through the upper crust. A plausible coupled mechanism is faults acting as fluid pressure «valves» during seismic slip (Sibson, 1990). This mechanism involves transient permeability on the fault during seismic slip, which is destroyed rather rapidly after rupture ceases. Possible self-sealing mechanisms of deformation include the crack-seal mechanism at higher temperatures (Ramsey and Huber, 1987), and by processes involving the creation, comminution, compaction or the dissolution and redeposition of fault gouge during fault slip and the associated cataclastic deformation (Blanpied *et al.*, 1992; Olsson, 1992). Simple dimensional calculations show that fault valving could dehydrate the crust without fluid supply from the mantle in 10^6-10^7 years, rising to 10^8-10^9 years when fluid supply from the subduction of oceanic crust is included (Nur and Walder, 1992). These calculations imply that an elevated pore pressure gradient could be maintained for long time periods over several thousand cycles of individual large earthquakes. In the «steady state» representing SOC, the upper crust would be held near criticality just below the stress required for macroscopic dynamic failure, as a coupled dynamic balance is formed between the fluid supply/discharge and tectonic strain energy input/release. This coupled mechanism is plausible since the percolation threshold for fluid flow is an exact map to the critical point (Bruce and Wallace, 1989).

4.2. *In a single cycle*

The valve action of faults is an example of positive feedback in the earthquake cycle, in the sense that the presence of fluid overpressure brings the overall system nearer failure (mechanical softening). This occurs because of a reduction in the effective stress $\sigma_e = \sigma - p$, where p is the pore pressure, moving the system nearer the composite Griffith-Coulomb failure envelope (fig. 5). Alternatively we may represent this as an increase in the relative crack extension force G/G_c. If the pore pressure is locally reduced, *e.g.* because of local dilatancy, then the system moves away from failure, representing a local negative feedback process (hardening), or a decrease in G/G_c. Figure 6a,b shows direct experimental evidence for the effect of changes in pore volume and pore-fluid pressure on the state of criticality in a single cycle of deformation, after Sammonds *et al.* (1992). In experiment (a) the pore fluid *pressure* in the sample volume was held constant by servo-control, representing defor-

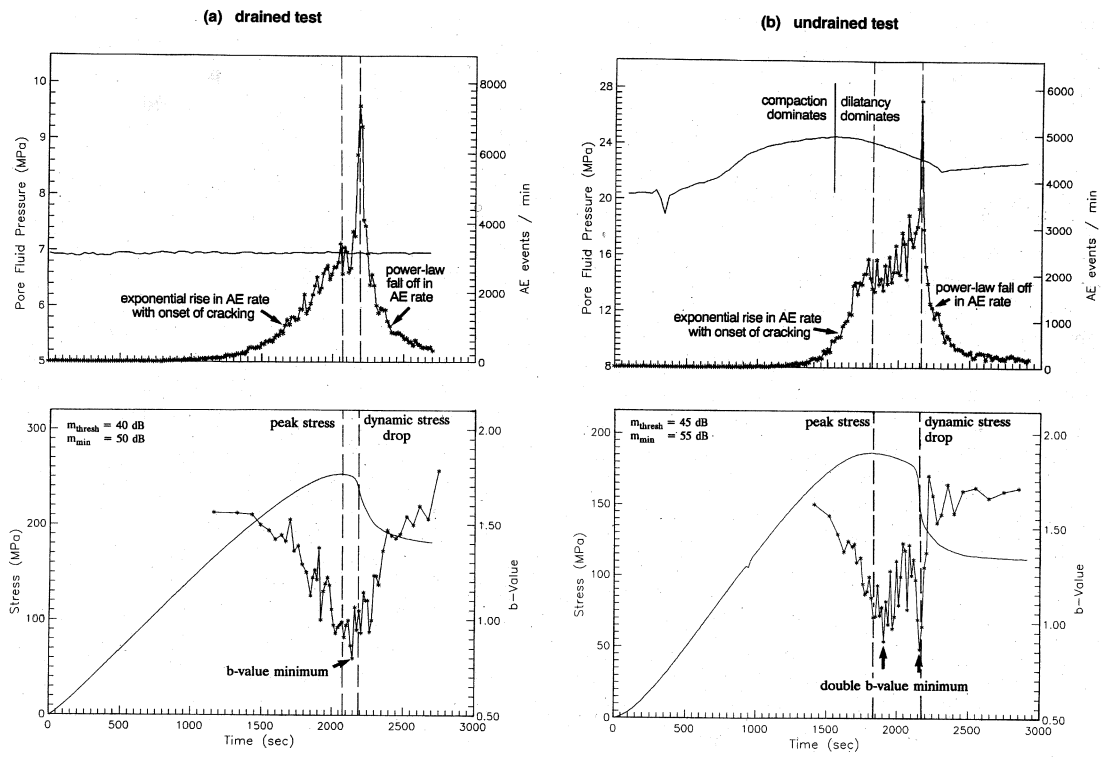

Fig. 6a,b. Laboratory results for the compressional failure of an intact specimen of Darley-dale sandstone under conditions of (a) constant pore fluid pressure and (b) constant pore fluid mass, after Sammonds *et al.* (1992). In each case the upper diagram shows the applied differential stress $\sigma_1 - \sigma_3$ and the pore fluid pressure p, and the lower diagram shows precursory fluctuations in the seismic event rate and the b-value calculated by the maximum likelihood (entropy) technique from the recorded acoustic emissions. Note that local dilatancy extends the strain softening phase, marked by the vertical dashed lines, and leads to an temporary increase in b-value.

mation in relatively permeable or «drained» conditions. In experiment (b) the pore fluid *mass* in the sample volume was held constant, representing relatively impermeable or «undrained» conditions. In undrained conditions the pore pressure initially rises due to compaction of the sample and a reduction in pore space, and then declines as local dilatancy due to microcracking creates new voids within the rock sample for the overpressured fluid to drain into. The phase of inferred dilatancy is marked by a sharp deceleration in acoustic emission event rate, a temporary increase in b-value, and delayed failure compared to the «drained» test – all aspects of the «negative feedback» of crack-opening displacement in relatively impermeable rock in a compressional stress field. Local dilatancy might also be expected on initially mated fault surfaces during the initial stages of slip (Rudnicki and Chen, 1988). With the exception of the model presented here, this local hardening effect has not yet been included in cellular automata modelling earthquakes.

In addition to these purely mechanical effects, time-dependent stress corrosion reactions

may produce accelerating crack growth because of a reduction in the energy required to propagate a crack by the physico-chemical weakening of material at the crack tip. For example quartz is substantially weakened by aqueous fluids of alkaline or neutral composition (Atkinson and Meredith, 1987), and there is good geological evidence for the occurrence of stress corrosion reactions at earthquake nucleation depths (Kerrich *et al.*, 1981). As G/G_c increases (because of mechanical weakening through decreased G_c, or increased G due to accelerated crack growth) a positive feedback may be introduced into the local physics of crack growth, eventually leading to instability even under constant external loading (Das and Scholz, 1981). Such time-dependent crack growth has been applied as a local mechanism of failure in a statistical model of earthquake foreshocks incorporating geological heterogeneity by Sornette *et al.* (1992).

5. Modelling the effect of fluids on the state of criticality in a single cycle

In this section we summarise the results from a model which attempts to incorporate the effect of fluids on earthquake statistics over a single cycle of macroscopic failure (Henderson *et al.*, 1994). We do not solve the complete poroelastic problem, but instead apply local rules from a damage mechanics formulation to approximate the effects of positive and negative feedback on crack growth on a 2-D cellular automaton. We use a square grid of elements with interactions between the four lateral and four diagonal neighbours taken into account. For small cracks of semilength c (representing either crack opening or a small amount of in-plane shear displacement) we might expect a growth rule of the form (Costin, 1983):

$$K \approx \sigma \frac{d-c}{d} \sqrt{(\pi c)} \qquad (5.1)$$

where K is the stress intensity (proportional to the square root of the crack extension force G; Atkinson, 1987), and d is the size of a characteristic «domain» of time-dependent stress relaxation or dilatant hardening due to the fluid-rock interactions described above. Once the crack has nucleated the stress intensity K (and hence the velocity of crack growth) eventually decreases with increasing crack length c. This local negative feedback leads to a reduced probability of future failure at that site, making it more likely that the next event will occur at a different nucleation site. Eventually the sample becomes peppered with a distributed array of fractures where there is a strong possibility of crack-crack interaction and coalescence. For example for a periodic array of cracks of semilength c and centre-centre spacing r

$$K \approx \sigma \sqrt{\left(r \tan \frac{\pi c}{2r} \right)} \qquad (5.2)$$

(Koiter, 1959; Rudnicki and Kanamori, 1981). Here the crack growth rule always has the form of a positive feedback between crack growth and an increase in stress intensity or crack growth velocity, leading to a runaway instability as $c \rightarrow r$. In the cellular automaton we approximate these rules by updating the local effective fracture toughness for a unit time step of the form $K_c(t_{i+1}) = f(n) K_c(t_i)$ where

$$f(n) = 1 \qquad : n = 0$$

$$f(n) = \left\{ 1 + \rho e^{\left(\frac{n-4}{20} \right)} \right\} e^{\left(\frac{-n^2}{16} \right)} \qquad : n = 1, 8 \qquad (5.3)$$

where n is the number of failed elements surrounding the given square, and $\rho > 0$ is an arbitrary negative feedback parameter which increases with local hardening or stress relaxation. As n increases $f(n)$ first increases up to a maximum at 1-2 elements for $0 < \rho < 5$ and then decreases, leading to a transition from local negative feedback ($f > 1$) to positive feedback ($f \ll 1$) in the local mechanics (Henderson *et al.*, 1994). The empirical factors 4, 16 and 20 were taken as constant, and were chosen to reflect a maximum local hardening factor $f = 4$

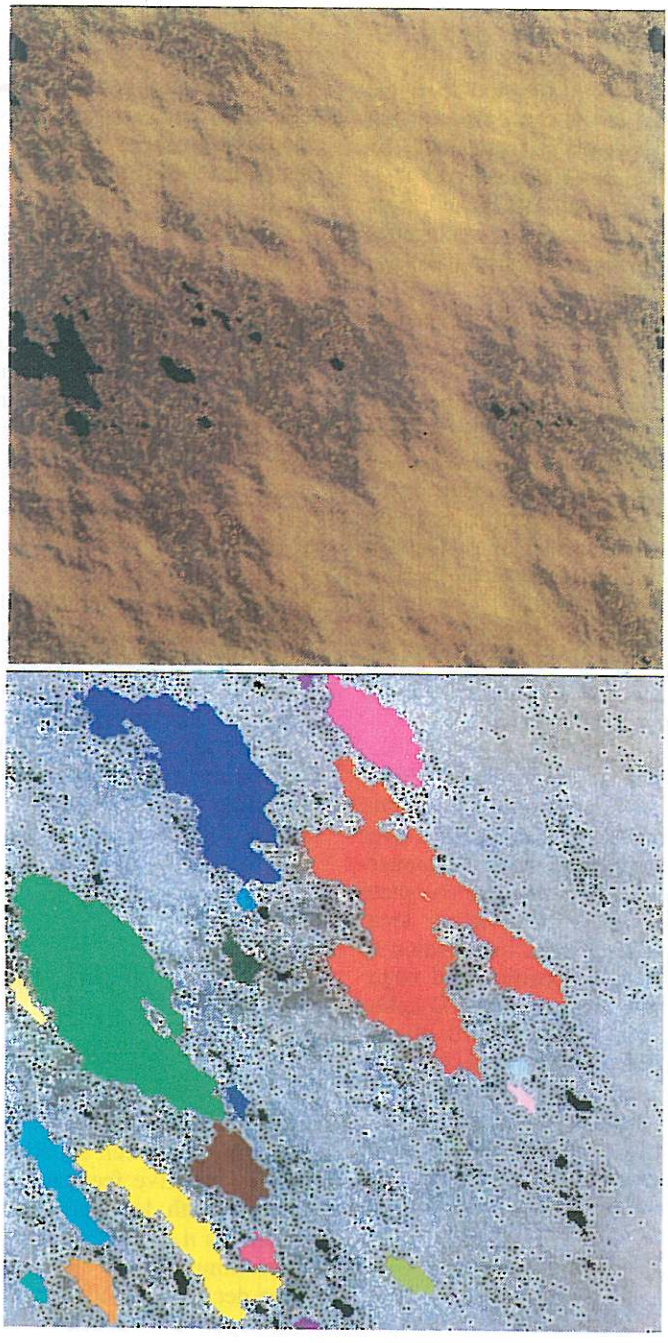

Fig. 7. Upper diagram: a snapshot of a fracture mechanics model for failure using the local rules of positive and negative feedback described in the main text. The fracture toughness field $K_c\,(i, j)$ is shown in tones of orange, with lighter shades implying tougher elements, and broken elements are shown in black. Lower diagram: illustration of the use of a CM subroutine to count the fracture areas, shown here in different colours.

for 1-2 failed neighbours with $0 < \rho < 5$, and a maximum softening factor of $f = 0$ for 8 failed neighbours, irrespective of ρ. The feedback function $f(n)$ has the property of decreasing K/K_c for small, isolated crack elements in the cellular automaton, but increasing K/K_c for larger cracks. As such $f(n)$ provides a qualitative behaviour grossly similar to (5.1) and (5.2), but does not reproduce all of the important aspects of crack-induced stress, such as anisotropic stress concentration at crack tips in cracks with low aspect ratio (our model has isotropic properties, apart from the effect of the square grid). At this stage of modelling, the feedback parameter also applies ony to a maximum of 8 nearest neighbours, and does not include long-range interactions. As such our mechanical model, in common with all cellular automata, are consistent only with the gross properties of the dynamical system, their main advantage being the more realistic degree of complexity allowed. Here the fracture toughness field is initialised to a random fractal distribution, to account for the known scale-invariance of geological heterogeneity, and the stress increased uniformly across the 2-D surface in each time step. Once an element fails ($K/K_c > 1$) it remains failed. In this respect the model applies only to a single cycle of failure, or to time steps short compared to the healing time for strength recovery across fault or crack surfaces. Apart from the crucial difference of the feedback rules for local fracture, the model is similar to that of Huang and Turcotte (1988).

Figure 7 (upper diagram) shows a snapshot of the early stages of damage in this model with increasing stress, for a cellular automaton comprising a grid of 512 by 512 nodes, a calculation made possible in reasonable timescales by using a multiply parallel computer (a Connection Machine CM-200) using a parallel programming language (CM FORTRAN). The toughness field is shown in tones of orange, with brighter shades representing tougher elements. Individual cracks (failed elements) are shown in black, and comprise a population of coexisting small isolated cracks and larger fractures formed by crack coalescence. The isolated cracks are surrounded by bright «halos» representing a local hardening or increase in effective toughness for $\rho > 0$, whereas the larger cracks are surrounded by darker shades representing softening due to stress concentration. Although the physics of crack propagation (eqs. (5.1), (5.2)) is only approximated by the local rules (5.3), the model pattern of distributed damage appears realistic compared to natural in-plane fracture systems because the large number of elements in the fracture toughness field allows the geological and mechanically-induced complexity of the system to be modelled adequately. The lower diagram of fig. 7 gives an example of a CM subroutine which has been used to identify individual connected clusters by assigning the highest initial toughness to a set of connected failed elements by a recursive comparison of nearest neighbours. This common number is used to display the clusters in different colours, and can be used to characterise the spatial statistics of the fracture set (*i.e.* the *b*-value and fractal capacity dimension).

Figure 8 shows the effect of increasing negative feedback (increased ρ) on the frequency-magnitude distribution, assuming that magnitude m scales logarithmically with the connected fault area A of an individual cluster ($m \approx \log A$). The effect of increased ρ is exactly analogous to increasing dissipation (decreasing α) in the non-conservative cellular automaton model of Olami *et al.* (1992). The negative correlation between locally increased K/K_c (obtained by decreasing ρ or increasing $-\rho$) and the seismic *b*-value is similar to that seen in the examples given in fig. 4a-c where fluid-rock interactions are known to be active. Figure 9 shows how the *b*-value changes with time as the driving stress is increased for different values of ρ. For $\rho = 0$ (local positive feedback only) the *b*-value decreases rapidly and monotonically, similar to the model of Huang and Turcotte (1989) and exactly as observed in the later stages of the «drained» test shown in fig. 6a. However for increased ρ (increased local negative feedback) failure is progressively delayed, and a temporary increase in *b*-value is observed, similar to the «undrained» test in fig. 6b, where dilatancy hardening is independently known to be the local mechanism

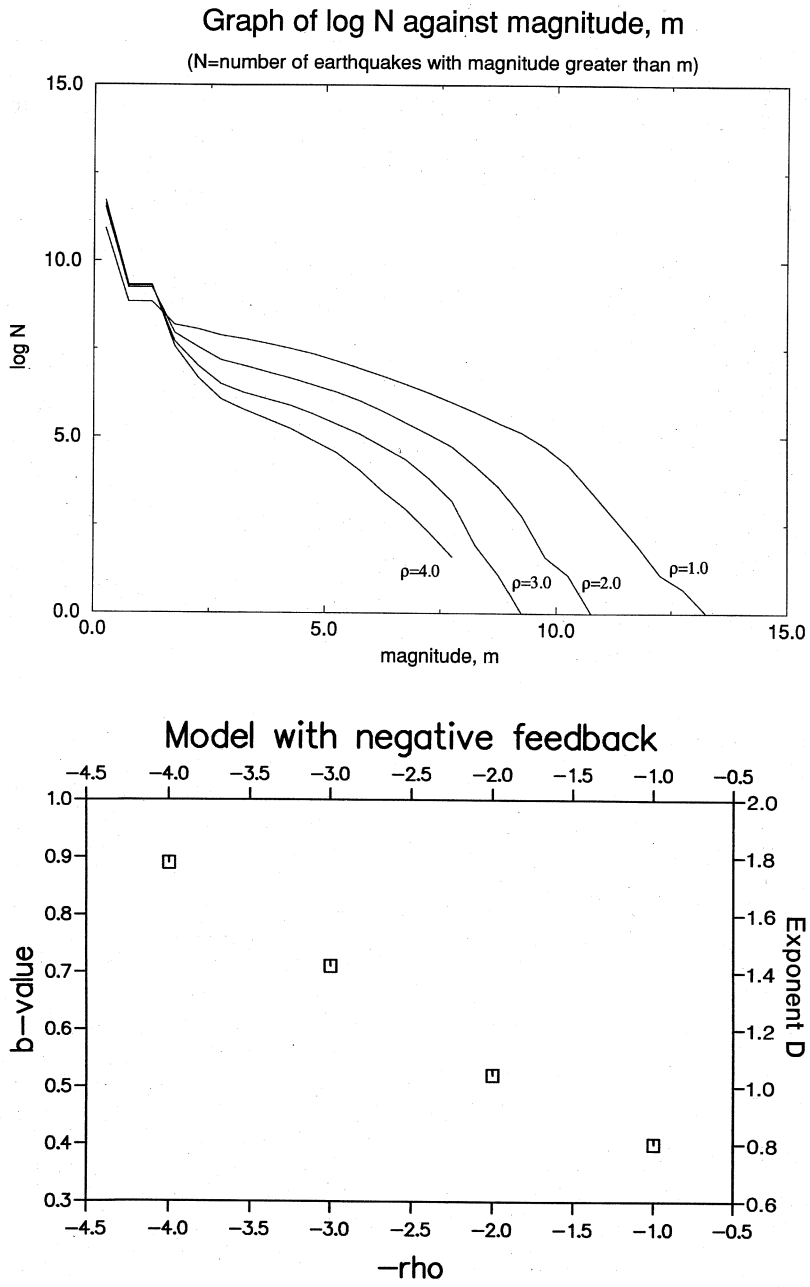

Fig. 8. Average statistical properties of the model at the same remote stress level for different values of the feedback parameter ρ. Upper diagram: the predicted frequency-magnitude statistics. All models exhibit a characteristic peak at low magnitudes, a fall-off at high magnitudes and fractal behaviour in the intermediate range. Lower diagram: variation in the seismic b-value with increasing levels of force conservation (lower ρ or higher $-\rho$). This diagram may be compared to results from the cellular automaton of Olami *et al.* (1992).

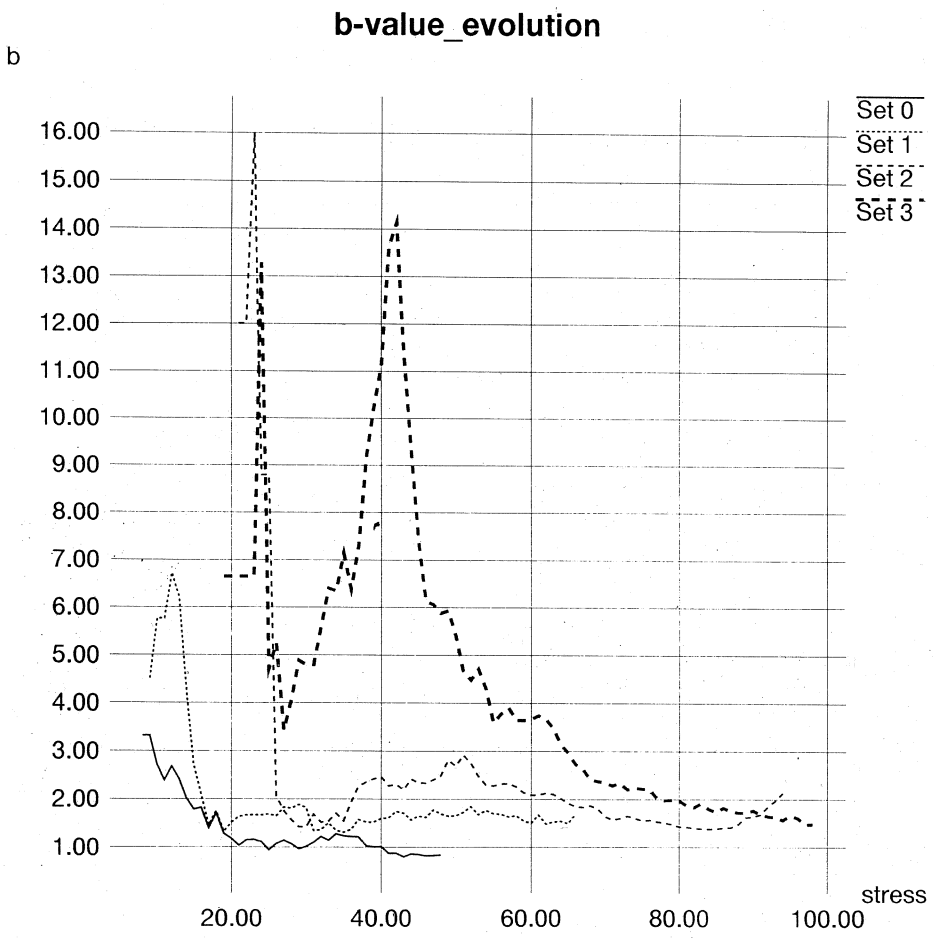

Fig. 9. Fluctuations in model seismic b-value in response to increasing external stress for different ρ. For no local negative feedback ($\rho = 0$) the b-value decreases with increasing stress, similar to the results of fig. 6a. For finite negative feedback ($\rho > 0$) the b-value shows a temporary increase, followed by a sharp decrease, similar to the results of fig. 6b.

of negative feedback. At earthquake nucleation depths fault rocks are likely to be generally relatively impermeable, exhibiting transient permeability only at the time of failure, so that the undrained tests (implying $\rho > 0$) are more likely to be realistic. A precursory pattern of increasing b-value followed by a short-term decrease has indeed been observed prior to a large number of earthquakes with varying degrees of statistical significance (Smith, 1980, 1986; Meredith *et al.*, 1990). Figure 6b is the only observation we are aware of a precursory increase/decrease in b due to pore fluid effects in laboratory tests, made possible only by the recent advent of good independent servo-control on the strain rate and pore fluid pressure or mass in the rock sample. These conditions are essential for reproducing the conditions of strain softening under relatively undrained conditions applicable in the Earth over much longer timescales.

6. Local dilatancy and small-scale characteristic effects

In the introduction we concentrated on variations in the frequency-magnitude distribution at intermediate and high magnitude. The results of figs. 7 and 8 suggest that the low-magnitude end of the distribution may also take on a form different from the Gutenberg-Richter law. Lomnitz-Adler (1985) modelled earthquakes as a percolation process involving a bimodal population of «strong» and «weak» asperities, and found a characteristic peak at both high and low magnitudes (corresponding respectively to the «percolation cluster», limited by the finite size of the model, and to the model cell size). In contrast Rundle (1993) showed that the finite thickness of the anelastic zone around a fault plane also leads to a characteristic size effect, but with a reduction in the frequency at low magnitudes relative to the Gutenberg-Richter law. Thus the low magnitude end of the distribution could in practice have a similar range of behaviour to that shown in fig. 3a-c at high magnitudes. In our model there is a characteristic peak at low magnitudes due to the influence of a local rule of negative feedback, corresponding to a domain size d between 1-2 elements, depending on the value of ρ.

It is important to emphasise that in our model dilatancy or time-dependent stress relaxation is a *local* phenomenon, the effect being to introduce a «grain» scale slightly larger than the cell size for $\rho > 0$. The model shows that such local laboratory-derived constitutive rules need not be expected to apply on simple renormalisation to a larger scale, mainly due to the degree of complexity involved. For example the dilatancy-diffusion model for earthquake precursors (Scholz *et al.*, 1973) is a classical case of a linear extrapolation of laboratory results which appears to be inappropriate on a crustal scale, even though it is confirmed even for the most recent laboratory tests (fig. 6b). In any case we await the arrival of more recordings of seismicity under improved signal/noise ratios for small earthquakes from deep borehole sites (*e.g.* Abercrombie and Leary, 1993) in order to examine any low-magnitude «characteristic» behaviour more closely, before any further modelling of how such effects may underpin the behaviour observed on a larger scale.

7. Discussion: implications for seismic hazard analysis

The various models and results described above leave open the question of the predictability of individual earthquakes. Over a single cycle we have shown theoretically and experimentally that pore-fluid effects may lead to systematic precursors to macroscopic failure under conditions of strong annealed heterogeneity and total stress drop. Shaw, Carlson and Langer (1992) have even produced models without either where coherent precursors are nevertheless generated. However the data on which such behaviour can be tested for large earthquakes is often still suggestive, and few statistical analyses of global data sets are available to test if individual earthquake precursors reported in the literature are not just the result of a judicious or fortuitous choice of data sets – which may contain inherently large fluctuations over short timescales precisely because of the critical nature of the process. The main problem remains the lack of good-quality observations of precursors on which to test any model for systematic precursors to large earthquakes (Scholz, 1990).

However the implications for seismic hazard analysis are much clearer. The first and most important assumption in any seismic hazard analysis is that the average properties of past record of instrumental, historical and palaeoseismic data is a good predictor of the future recurrence. This assumption of «stationarity» now has a sound physical basis if earthquakes are a SOC phenomenon – *i.e.* the steady-state of criticality is represented by a dynamic equilibrium over several earthquake cycles of strain energy input and dissipation (and as we have argued coupled to pore fluid input and flux). Thus it is extremely important to use as long a record as possible in predicting the future hazard, preferably involving several cycles and palaeoseismic data. A type example

of SOC emerging from a statistical mechanical model with known moment release rate compared to such a long-term data set is Southern California (fig. 3b, after Main and Burton, 1984), where an extrapolation of short-term instrumental data confined by the observed seismotectonic slip rate using eqs. (2.11) and (2.12) produced a good match with the independently-derived palaeoseismic recurrence found by Sieh (1978). The recent models for criticality in the Earth described in the introduction show that such a «maximum entropy» or «information theory» approach now has a wider physical justification, exactly analogous to the equivalence established by Jaynes (1957) between information theory and statistical mechanics in thermodynamic systems.

Figure 3a-c throws up an interesting possibility of the rather subjective choice of seismotectonic area having a strong influence on the form of the frequency-magnitude distribution, with large areas typically exhibiting an exponential tail to the distribution, medium-sized areas exhibiting fractal statistics, and small areas concentrated around particular faults having a characteristic peak at high magnitudes. It is well known that different experts habitually choose different schemes for seismic zoning in earthquake hazard analysis (*e.g.* Reiter, 1991), but not that such a subjective choice may strongly influence the form of the frequency-magnitude distribution.

8. Conclusions

Pore fluids exert a strong mechanical and chemical influence on the local constitutive laws and scaling exponents during single cycles of rock deformation in the laboratory. Fluid-rock interactions are also known to be important in transient man-made «experiments» conducted at an intermediate scale during hydraulic mining, dam impoundment and hydrocarbon extraction. Even though such constitutive laws do not necessarily scale simply to a crustal level the geological and geochemical record is replete with independent evidence for the mechanical and chemical influence of pore fluids on the development of faults and fractures on an outcrop scale. In all cases the fluid-rock interactions are strongly coupled to the mechanical behaviour of the sample on a macroscopic scale through competing mechanisms of positive and negative feedback (respectively hardening or softening processes) not yet commonly found in cellular automata modelling earthquakes. In particular the valve action of faults as intermittent pressure seals may persist over several thousand earthquake cycles, so fluids may be an important self-tuning mechanism for criticality in the earth's upper crust, even though their presence is not explicitly required to produce SOC. Implicitly most successful models of SOC apply an empirical but arbitrary dissipative parameter which we have shown has the same effect as pore fluid-related feedback mechanisms would have on varying the Gutenberg-Richter *b*-value. For example even the preliminary model presented here reproduces the observed negative correlation between increasing normalised crack extension force and seismic *b*-value found for stress corrosion in tensile laboratory tests, in undrained compressional tests and during hydraulic mining-induced seismicity. For finite negative feedback due to local dilatancy hardening or time-dependent stress relaxation, the model predicts the observed temporary increase in *b*-value observed during undrained laboratory tests and as a precursor to several crustal-scale earthquakes.

Acknowledgements

The experimental work described above was funded by NERC grant number GR3/6812, and the fracture modelling was carried out on a CM200 at the Edinburgh Parallel Computing Centre. We are grateful for the constructive review of an anonymous referee, whose comments resulted in significant improvements in the final text. During the writing of this paper we learned with sadness of the death of Jorge Lomnitz-Adler. Jorge was a pioneer of the application of statistical mechanics and percolation theory to earthquakes, and some of the ideas described above were developed against a background of lively correspondence or dis-

cussion with him ongoing since the early eighties. He was a genuine «good guy», and we shall miss his enthusiasm, insight and good humour.

REFERENCES

ABERCROMBIE, R. and P. LEARY (1993): Source parameters of small earthquakes recorded at 2.5 km depth, Cajon pass, Southern California: implications for earthquake scaling, *Geophys. Res. Lett.*, **20**, 1511-1514.

ATKINSON, B.K. (1987): Introduction to fracture mechanics and its geophysical applications, in *Fracture Mechanics of Rock*, edited by B.K. ATKINSON (Academic Press, London), 1-26.

ATKINSON, B.K. and P.G. MEREDITH (1987): The theory of subcritical crack growth with applications to minerals and rocks, in *Fracture Mechanics of Rock*, edited by B.K. ATKINSON (Academic Press, London), 111-166.

BAK, P. and C. TANG (1989): Earthquakes as a self-organized critical phenomenon, *J. Geophys. Res.*, **94**, 15635-15637.

BARENBLATT, G. I. (1962): The mathematical theory of equilibrium cracks, *Adv. App. Mech.*, **7**, 55-129.

BEN-ZION, Y. and J.R. RICE (1993): Earthquake failure sequences along a cellular fault zone in a three-dimensional elastic solid containing asperity and non-asperity regions, *J. Geophys. Res.*, **98**, 14109-14131.

BLANPIED, M.L., D.A. LOCKNER and J.D. BYERLEE (1992): An earthquake mechanism based on rapid sealing of faults, *Nature*, **358**, 574-576.

BRUCE, A. and D. WALLACE (1989): Critical point phenomena: universal physics at large length scales, in *The New Physics*, edited by P. DAVIES (Cambridge University Press), 236-267.

BURRIDGE, R. and L. KNOPOFF (1967): Model and theoretical seismicity, *Bull. Seismol. Soc. Am.*, **57**, 341-371.

CARLSON, J.M. and J.S. LANGER (1989): Mechanical model of an earthquake fault, *Phys. Rev.*, **A 40**, 6470-6484.

CARLSON, J.M., E.R. GRANNAN, C. SINGH and G.H. SWINDLE (1993): Fluctuations in self-organizing systems, *Phys. Rev.*, **E 48**, 688-698.

CEVA, H. (1993): From self-organized criticality to first-order-like behaviour: a new type of percolative transition, *Phys. Rev.*, **E 48**, 157-160.

CHESTER, F., J.P. EVANS and R.L. BIEGEL (1993): Internal structure and weakening mechanisms of the San Andreas fault, *J. Geophys. Res.*, **98**, 771-786.

COSTIN, L.S. (1983): A microcrack model for the deformation and failure of rock, *J. Geophys. Res.*, **88**, 9485-9492.

DAS, S. and C.H. SCHOLZ (1981): Theory of time-dependent rupture in the earth, *J. Geophys. Res.*, **86**, 6039-6051.

HENDERSON, J., I. MAIN, P. MEREDITH and P. SAMMONDS (1992): The evolution of seismicity at Parkfield, observation, experiment and a fracture-mechanical interpretation, *J. Struct. Geol.*, **14**, 905-913.

HENDERSON, J., C. MACLEAN, I. MAIN and M. NORMAN (1994): A fracture-mechanical cellular-automaton model of seismicity, *PAGEOPH*, **142**, 545-566.

HODGKINS, M.A. and K.G. STEWART (1994): The use of fluid inclusions to constrain fault zone overpressure, temperature and kinematic history: an example from the Alpi Apuane, Italy, *J. Struct. Geol.*, **16**, 85-96.

HUANG, J. and D.L. TURCOTTE (1988): Fractal distribution of stress and strength and variations of *b*-value, *Earth Planet. Sci. Lett.*, **91**, 223-230.

JAYNES, E.T. (1957): Information theory and statistical mechanics, *Phys. Rev.*, **106**, 620-630.

JIN, A. and K. AKI (1986): Temporal change in coda *Q* before the Tangshan earthquake of 1976 and the Haicheng earthquake of 1975, *J. Geophys. Res.*, **91**, 665-673.

KAGAN, Y.Y. (1993): Statistics of characteristic earthquakes, *Bull Seismol. Soc. Am.*, **83**, 7-24.

KANAMORI, H. (1978): Quantification of earthquakes, *Nature*, **271**, 411-414.

KELLER, E.A. and H.A. LOACIGA (1993): Fluid-pressure induced seismicity at regional scales, *Geophys. Res. Lett.*, **20**, 1683-1686.

KERRICH, R. (1986): Fluid infiltration into fault zones: chemical, isotopic and mechanical effects, *PAGEOPH*, **124**, 225-268.

KERRICH, R., T.E. LA TOUR and R.L. BARNETT (1981): Mineral reactions in intragranular fracture propagation: implications for stress corrosion cracking, *J. Struct. Geol.*, **3**, 77-87.

KOITER, W.T. (1959): An infinite row of collinear cracks in an infinite elastic sheet, *Ing. Arch.*, **28**, 168-172.

LOMNITZ-ADLER, J. (1985): Asperity models and characteristic earthquakes, *Geophys. J.R. Astr. Soc.*, **83**, 435-450.

LOMNITZ-ADLER, J. (1988): The theoretical seismicity of asperity models: an application to the coast of Oaxaca, *Geophys. J.*, **95**, 491-501.

LOMNITZ-ADLER, J. (1993): Automaton models of seismic fracture: constraints imposed by the magnitude-frequency relation, *J. Geophys. Res.*, **98**, 17745-17756.

MAIN, I.G. (1987): A characteristic earthquake model of the seismicity preceding the eruption of Mount St. Helens on 18 May 1980, *Phys. Earth Planet. Int.*, **49**, 283-293.

MAIN, I.G. (1991): A modified Griffith criterion for the evolution of damage with a fractal distribution of crack lengths: application to seismic event rates and *b* values, *Geophys. J. Int.*, **107**, 353-362.

MAIN, I.G. (1992): Earthquake scaling, *Nature*, **357**, 27-28.

MAIN, I.G. and P.W. BURTON (1984): Information theory and the earthquake frequency-magnitude distribution, *Bull. Seismol. Soc. Am.*, **74**, 1409-1426.

MAIN, I.G. and P.W. BURTON (1986): Long-term earthquake recurrence constrained by tectonic seismic moment release rates, *Bull. Seismol. Soc. Am.*, **76**, 297-304.

MAIN, I.G., P.R. SAMMONDS and P.G. MEREDITH (1993): Application of a modified Griffith criterion to the evolution of fractal damage during compressional rock failure, *Geophys. J. Int.*, **115**, 367-380.

MAIN, I.G., J.R. HENDERSON, P.G. MEREDITH and P.R. SAMMONDS (1994): Self-organised criticality and fluid-rock interactions in the brittle field, *PAGEOPH*, **142**, 529-544.

MANDL, F. (1988): *Statistical Physics* (Wiley, New York), 2nd ed.

MEREDITH, P.G. and B.K. ATKINSON (1983): Stress corrosion and acoustic emission during tensile crack propagation in Whin Sill dolerite and other basic rocks, *Geophys. J.R. Astr. Soc.*, **75**, 1-21.

MEREDITH, P.G., I.G. MAIN and C. JONES (1990): Temporal variations in seismicity during quasi-static and dynamic rock failure, *Tectonophysics*, **175**, 249-268.

NUR, A. and J. WALDER (1992): Hydraulic pulses in the Earth's crust, in *Fault Mechanisms and Transport properties in Rocks*, edited by B. EVANS and T.F. WONG (Academic Press, London), 461-473.

OLAMI, Z., H.J.S. FEDER and K. CHRISTENSEN (1992): Self-organized criticality in a continuous, non-conservative cellular automaton modelling earthquakes, *Phys. Rev. Lett.*, **68**, 1244-1247.

OLSSON, W.A. (1992): The effect of slip on the flow of fluid through a fracture, *Geophys. Res. Lett.*, **19**, 541-543.

RAMSEY, J.G. and M. I. HUBER (1987): *The Techniques of Modern Structural Geology* (Academic Press, London), vol. 2.

REITER, L. (1991): *Earthquake Hazard Analysis* (Columbia University Press, New York).

RICE, J.R. (1992): Fault stress state, pore pressure distributions and the weakness of the San Andreas fault, in *Fault Mechanisms and Transport Properties in Rocks*, edited by B. EVANS and T.F. WONG (Academic Press, London), 475-503.

RUDNICKI, J.W. and H. KANAMORI (1981): Effect of fault interaction on moment, stress drop and strain energy return, *J. Geophys. Res.*, **86**, 1785-1793.

RUDNICKI, J.W. and C.-H. CHEN (1988): Stabilization of rapid frictional slip on a weakened fault by dilatant hardening, *J. Geophys. Res.*, **93**, 4745-4757.

RUNDLE, J.B. (1989): Derivation of the complete Gutenberg-Richter magnitude-frequency relation using the principle of scale-invariance, *J. Geophys. Res.*, **94**, 12337-12342.

RUNDLE, J.B. (1993): Magnitude-frequency relations for earthquakes using a statistical mechanical approach, *J. Geophys. Res.*, **98**, 21943-21949.

RUNDLE, J.B. and W. KLEIN (1993): Scaling and critical phenomena in a cellular automaton slider-block model for earthquakes, *J. Stat. Phys.*, **72**, 405-413.

SAMMONDS, P.R., P.G. MEREDITH and I.G. MAIN (1992): Role of pore fluids in the generation of seismic precursors to shear fracture, *Nature*, **359**, 228-230.

SATO, K., T. ISOBE, N. MORI and T. GOTO (1986): Microseismic activity associated with hydraulic mining, *Int. J. Rock Mech. Min. Sci. and Geomech. Abstr.*, **23**, 85-94.

SCHOLZ, C.H. (1990): *The mechanics of Earthquakes and Faulting* (Cambridge University Press, Cambridge).

SCHOLZ, C.H., L.R. SYKES and Y.P. AGGARWAL (1973): Earthquake prediction: a physical basis, *Science*, **181**, 803-810.

SCHWARTZ, D.P. and K.J. COPPERSMITH (1984): Fault behaviour and characteristic earthquakes: examples from the Wasatch and the San Andreas fault zones, *J. Geophys. Res.*, **89**, 5681-5698.

SEGALL, P. (1989): Earthquakes triggered by fluid extraction, *Geology*, **17**, 942-946.

SIEH, K. (1978): Prehistoric large earthquakes produced by slip on the San Andreas fault at Pallet Creek, California, *J. Geophys. Res.*, **83**, 3907-3939.

SHAW, B.E., J.M. CARLSON and J.S. LANGER (1992): Patterns of seismic activity preceding large earthquakes, *J. Geophys. Res.*, **97**, 479-488.

SIBSON, R.H. (1977): Fault rocks and fault mechanisms, *J. Geol. Soc. Lond.*, **133**, 191-214.

SIBSON, R.H. (1981): Fluid flow accompanying faulting: field evidence and models, in *Earthquake prediction, an International Review*, edited by D.W. SIMPSON and P.G. RICHARDS, Maurice Ewing Series, **4**, Washington DC, 593-603.

SIBSON, R.H. (1990): Conditions for fault valve behaviour, in *Deformation mechanisms, rheology and tectonics*, edited by R.J. KNIPE and E.H. RUTTER, Geol. Soc. London, special pub, **54**, 15-28.

SIBSON, R.H., F. ROBERT and K.H. POULSEN (1988): High-angle reverse faults, fluid-pressure cycling, and mesothermal gold-quartz deposits, *Geology*, **16**, 551-555.

SMITH, W.D. (1980): The *b*-value as an earthquake precursor, *Nature*, **289**, 136-139.

SMITH, W.D. (1986): Evidence for precursory changes in the frequency-magnitude *b*-value, *Geophys. J.R. Astr. Soc.*, **86**, 815-838.

SORNETTE, A. and D. SORNETTE (1989): Self-organized criticality and earthquakes, *Europhys. Lett.*, **9**, 197-202.

SORNETTE, D., C. VANNESTE and L. KNOPOFF (1992): Statistical models of earthquake foreshocks, *Phys. Rev.*, **A 45**, 8351-8357.

SORNETTE, D., P. COWIE, P. MILTENBERGER, A. SORNETTE and C. VANNESTE (1994a): Organization of rupture, *Solid State Phenomena*, **35**, 303-318.

SORNETTE, D., P. MILTENBERGER and C. VANNESTE (1994b): Statistical physics of fault patterns self-organised by repeated earthquakes, *Pure App. Geophys.*, 491-528.

STAUFFER, D. (1985): *Introduction to Percolation Theory* (Taylor and Francis, Philadelphia).

WARD, S.N. (1992): An application of synthetic seismicity in earthquake statistics: the middle America trench, *J. Geophys. Res.*, **97**, 6675-6682.

XIE, H. and W.G. PARISEAU (1991): Studies on mechanism of rock burst-associated seismicity mines by using fractals and damage mechanics, in *Rock Mechanics: Proceedings of the 33rd US Symposium*, edited by J.R. TILLERSON and W.R. WAWERSIK, *Balkema, Rotterdam*, 745-754.